

## References

- <sup>1</sup>Glauert, H., "The Stability of a Body Towed by a Light Wire," R&M 1312, Feb. 1930, Aeronautical Research Committee, Farnborough, England.
- <sup>2</sup>Glauert, H., "The Form of a Heavy Flexible Cable Used for Towing a Heavy Body below an Aeroplane," R & M 1592, Feb. 1934, Aeronautical Research Committee, Farnborough, England.
- <sup>3</sup>O'Hara, F., "Extension of Glider Tow Cable Theory to Elastic Cables Subject to Air Forces of a Generalized Form," R & M 2334, Nov. 1945, Aeronautical Research Council, Farnborough, England.
- <sup>4</sup>Phillips, W. H., "Theoretical Analysis of Oscillations of a Towed Cable," TN 1796, 1949, NACA.
- <sup>5</sup>Etkin, B. and Mackworth, J. C., "Aerodynamic Instability of Non-Lifting Bodies Towed Beneath an Aircraft," TN 65, 1963, Institute of Aerophysics, University of Toronto, Toronto, Ontario, Canada.
- <sup>6</sup>Shanks, R. E., "Investigation of the Dynamic Stability and Controllability of a Towed Model of a Modified Half-Cone Reentry Vehicle," TN D-2517, 1965, NASA.
- <sup>7</sup>Shanks, R. E., "Experimental Investigation of the Dynamic Stability of a Towed Parawing Glider," TN D 1614, 1963, NASA.
- <sup>8</sup>Shanks, R. E., "Experimental Investigation of the Dynamic Stability of a Towed Parawing Glider Air Cargo Delivery System," TN D-2292, 1964, NASA.
- <sup>9</sup>Sohne, W., "Directional Stability of Towed Airplanes," TM 1401, 1956, NACA.
- <sup>10</sup>Reid, W. P., "Stability of a Towed Object," *SIAM Journal of Applied Mathematics*, Vol. 15, No. 1, Jan. 1967, pp. 1-2.
- <sup>11</sup>Huffman, R. R. and Genin, J., "The Dynamical Behaviour of a Flexible Cable in a Uniform Flow Field," *Aeronautical Quarterly*, Vol. XXII, Pt. 2, May 1971, pp. 183-195.
- <sup>12</sup>Casarella, M. J. and Parsons, M., "Cable Systems Under Hydrodynamic Loading," *MTS Journal*, Vol. 4, No. 4, 1970, pp. 27-44.
- <sup>13</sup>Sheldon, D. F., "A Study of the Stability of a Plate-Like Load Towed Beneath a Helicopter," *Journal of Mechanical Engineering Science*, Vol. 13, No. 5, 1971, pp. 330-343.
- <sup>14</sup>Szustak, L. S. and Jenny, D. S., "Control of Large Crane Helicopters," *Journal of the American Helicopter Society*, Vol. 16, No. 3, July 1971, pp. 11-22.
- <sup>15</sup>Hutto, A. J., "Qualitative Report on Flight Test of a Two-Point External Load Suspension System," Reprint 473, Presented at the 26th Annual National Forum of the American Helicopter Society, Washington, D.C.
- <sup>16</sup>Lehmann, J. W., "The Aerodynamics Characteristics of Non-Aerodynamic Shapes," M.S. thesis, GAM/AE/68-6, June 1968, School of Engineering, Air Force Institute of Technology, Wright-Patterson Air Force Base, Ohio.
- <sup>17</sup>Etkin, B., *Dynamics of Flight*, Wiley, New York, 1958, Chap. 4.

FEBRUARY 1973

J. AIRCRAFT

VOL. 10, NO. 2

## Far-Field Structure of Aircraft Wake Turbulence

W. H. Mason\* and J. F. Marchman III†

Virginia Polytechnic Institute and State University, Blacksburg, Va.

Detailed mean flow measurements were obtained at stations up to thirty chordlengths downstream in an airfoil trailing vortex using a yawhead pressure probe in the Virginia Tech Six-Foot Subsonic Tunnel. Mass injection at the wingtip was shown to hasten the vortex decay. A theoretical method has been developed to show the effect of wing circulation distribution on the structure of the outer portion of the vortex and excellent agreement with the experimental data is demonstrated.

## Nomenclature

$a$	= probe radius
$A_C$	= core radius
$A_n$	= coefficients of Fourier series of wing circulation
$AR$	= aspect ratio
$C$	= wing chord
$F$	= force between probe and vortex
$J_o$	= moment of inertia of flat sheet about plane of symmetry
$J_{y_1}$	= momental inertia of flat sheet about c.g.
$J_{r_1}$	= moment of inertia after rollup
$K$	= ratio of effective to kinematic viscosity
$\dot{m}$	= mass flow
$P_{st}$	= static pressure
$P_o$	= stagnation pressure
$\Delta P$	= pressure difference across yawhead probe tip
$Q$	= dynamic pressure
$r, \theta, z$	= cylindrical coordinate directions
$Re$	= Reynolds number
$t$	= time
$s$	= wing semispan
$V_x, V_y, V_z$	= Cartesian velocities
$V_r, V_\theta, V_z$	= cylindrical velocities

$V_\infty$	= freestream undisturbed velocity
$x, y, z$	= cartesian coordinate directions
$\bar{y}$	= c.g. of flat vorticity sheet
$\gamma$	= flat vorticity sheet strength
$\epsilon_T$	= wing-tip twist angle
$\lambda$	= wing taper ratio
$\nu_T$	= kinematic viscosity
$\nu^T$	= effective (turbulent) kinematic viscosity
$\rho$	= mass density

## Introduction

THE prediction of the turbulence trail of an aircraft has become extremely important with the introduction of "Jumbo Jet" class aircraft into terminal areas because of the potential hazard to other aircraft encountering them in flight. The FAA has initiated longer time spacing between large jet aircraft and following aircraft to assure safe separation and reduce the possibility of vortex encounter. This longer time spacing reduces the number of operations possible at busy airports and compounds the already serious traffic problem. In addition, even though the next generation of avionics is expected to allow aircraft to land and take off with significantly less spacing, wake turbulence could become the major limiting factor prohibiting the achievement of the maximum airport capacity afforded by improved equipment. Therefore, in order to minimize the wait time of aircraft on the ground and in the air, with its accompanying noise and chemical

Presented as Paper 72-40 at the AIAA 10th Aerospace Sciences Meeting, San Diego, Calif., January 17-19, 1972; submitted February 14, 1972; revision received December 14, 1972. This research was supported by NASA Grant NGL 47-004-067.

Index category: Aircraft Aerodynamics.

\*Graduate Student.

†Associate Professor, Associate Member AIAA.

pollution, the wake turbulence must be predicted accurately and reduced or eliminated if possible, allowing the most efficient use of present airport facilities.

Aircraft wake turbulence and trailing vortices have been the subject of many studies in the past, but most interest has centered on the effects near the aircraft such as the effects of the vortex and wake on the tail and control surfaces of the aircraft. The trailing vortex, as pictured in Fig. 1, is a result of the circulatory lifting flow on the aircraft wing. The classic Joukowski Theorem gives the relation between circulation and lift. Hence the large gross weights of the new aircraft can be expected to generate much larger circulation and thus larger, more intense trailing vortices.

Of the many investigations of the downwash behind the wing, only three studies have been made at a substantial number of chordlengths downstream in the fully developed trailing vortex. Fage and Simmons<sup>1</sup> (1925) conducted tests at up to 13 chordlengths downstream using a hot wire anemometer. Mowforth<sup>2</sup> has conducted experiments at up to 10 chordlengths downstream and attempted to make static pressure measurements. No velocity profiles were presented and the measurements were made with an extremely small wind tunnel and probe. Perhaps the experiment most similar to the present work was conducted by Gasparek<sup>3</sup> where measurements were made at chordlengths up to 8  $Z/C$ , beyond which he found it impossible to keep the probe in the vortex. Recent work using a larger model and freestream velocity has been done by Chigier and Corsiglia<sup>4</sup> using a hot wire probe, but only at distances up to four chordlengths downstream. The results show a velocity overshoot in the vortex core. It is interesting to note that the work done using hot wire probes show an axial velocity overshoot, while workers using pressure probes predict a velocity deficit in the core.

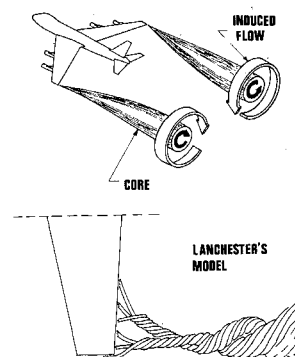
From the present work it can be concluded that this is due to the failure to account for static pressure variation in previous investigations. The present work presents the first measured static pressure distributions.

The theory of turbulent vortex cores is at best primitive, despite the fact that the trailing vortex is turbulent as is almost every real vortex. The simplest method of dealing with turbulent flows has been to employ the concept of an eddy viscosity in which the turbulent diffusivity is supposed to be directly proportional to the molecular viscosity. With this assumption the governing equations are reduced to the laminar case and the methods used for laminar flows can be applied to the turbulent case. Squire<sup>5</sup> gave the first solution using this concept, making the eddy viscosity proportional to the circulation at the plane of symmetry of the wing.

Further improvement on the theory can be achieved by using a different viscosity model for the flow in the axial direction. This approach has been used by Fernandez and Lubard<sup>6</sup> in an integral approach, with the results showing that adjustments of the initial conditions could cause singularities in the solution. These singularities are supposed to indicate conditions that would correspond to vortex breakdown. This is the theoretical justification for varying the initial conditions experimentally through mass injection. All of these theoretical and experimental efforts seem to indicate that vortex decay due to simple diffusion is one of the least rapid diffusion processes that occurs in free turbulent flows, hence the necessity to predict it accurately. Hoffman and Joubert<sup>7</sup> have used arguments similar to turbulent boundary layers in order to deduce a logarithmic distribution of circulation on the core.

Until recently, it has been supposed that the vortex exhibits a  $1/r$  "potential" type behavior immediately outside the vortex core. Donaldson<sup>8</sup> recently reviewed an early study by Betz<sup>9</sup> which shows that this is not the case and that the outer inviscid vortex depends on the circula-

Fig. 1 Illustration of trailing vortex.



tion distribution about the wing. Betz performed his calculations for the elliptic wing case and Donaldson was able to show that this theory describes the outer portion of the vortex much better than any theory which included viscosity effects. The present work extends this theory to include any wing planform that can be described using lifting line theory, showing the importance of the various parameters for the outer portion of the vortex.

### Experimental Investigation

The experimental study was conducted in the Virginia Tech Six-Foot Subsonic Wind Tunnel which has a test section 28 ft long. An NACA 0012 rectangular wing was placed at the test section front, allowing measuring stations of up to 30 chordlengths downstream. This wing was also modified to allow mass injection at the wing tip. Two wind-tunnel velocities were investigated, 70 fps and 100 fps, with mass injection employed only during the 70 fps case. The vortex was investigated by use of small 5-hole yawhead and static pressure probes. Pressures were measured on three inclined manometers and the probe orientations were measured by potentiometers, with readings recorded on a digital voltmeter. Some details of the apparatus, test procedure, and data reduction are given below.

The Virginia Tech Six-Foot Subsonic Wind Tunnel is a continuous, single-return, low turbulence, closed test-section tunnel. Standard calibrated manometers, barometers, and digital temperature gages are used to measure tunnel flow conditions.

An NACA 0012 straight, square-tipped wing was mounted vertically from the center of the tunnel roof one ft from the front of the test section. The mounting allowed the wing to be set at variable angles of attack and placed the free wing tip near the center of the wind tunnel. This mounting allowed placement of the traversing mechanism at up to 30 chordlengths behind the wing before the flow reached the diffuser section of the tunnel. The wing had a semispan of 4 ft, chord  $\frac{2}{3}$  ft, angle-of-attack  $7\frac{1}{2}^\circ$ , lift coefficient, 0.674, and Reynolds number of  $2.5 \times 10^5$ ,  $3.5 \times 10^5$ .

In order to include mass injection at the wing tip, the wing model was modified to carry a copper tube  $\frac{1}{4}$  in. in outside diameter along the leading edge and tip as shown in Fig. 2. Mass injection was obtained by metering air

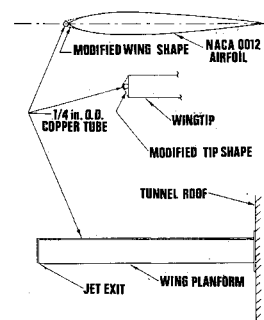


Fig. 2 Test wing.

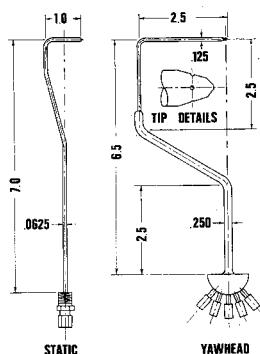


Fig. 3 Test probes.

from an available high pressure supply using a simple orifice metering system constructed according to ASME specifications. Jet operating conditions were  $2.15 \times 10^{-4}$ ,  $3.8 \times 10^{-4}$  slugs/sec. The wing was tested on the tunnel's mechanical balance system for comparison of the wing lift and drag coefficients with and without mass injection and the results indicated that injection had a negligible effect on wing aerodynamics.

The probe mechanism used in this study employed an existing traverse that provided a vertical translation movement of 4 ft. Added to the basic assembly was an adapter unit that allowed a probe to rotate in pitch and yaw around its point. It was designed so as to be rigid in intensely swirling flows while presenting minimum disturbance to the flowfield at the point of the probe. Throughout the tests no vibration of any probe could be detected visually, insuring accurate pressure measurements. Rotation in pitch is accomplished by a machined steel arc and track which allowed a rotation of  $34^\circ$  at the probe point. Rotation in yaw is accomplished by design of any probe attached to the system such that the point of the probe is above its shaft, as shown in Fig. 3, so that it is free to rotate about its shaft. Probe position in both planes of motion was determined from voltage readings taken from potentiometers connected to each drive mechanism.

The  $\frac{1}{8}$  in. outside diameter 5 hole yawhead probe used in the investigation was custom built for the experiment by United Sensor Corp. as shown in Fig. 3. By measuring pressure differences between opposite holes in the same plane the angle of flow can be determined. The probe showed a linear response over a range of  $\pm 10^\circ$ . The  $\frac{1}{16}$  in. o.d. static probe used in the experiment was also made by United Sensor Corp. This probe, also shown in Fig. 3, has a much smaller area than the yawhead probe. All probe pressures were read on inclined manometers which were carefully calibrated and designed for the small pressure ranges of the present tests.

The procedure used for the investigation of the trailing vortex was straight forward. All the information necessary from the yawhead probe was obtained and then the same series of tests was conducted using the static probe. Initially at each station the vortex center was found by raising the probe until the yaw angle of the flow was found to be zero, and then the traverse was moved laterally in the test section until the pitch angle was found to be zero. Because of symmetry the vortex center will occur where both the pitch and yaw angles are zero. Once the vortex center was found, a vertical traverse was made starting from the center and going 4 in. above the center (approximately 8 core radii), and then returning to the center and traveling 4 in. below the vortex center. Originally it was planned to align the probe so that there was no flow angularity relative to the flow but it was found that moving the probe in the vortex caused the vortex to move. For example, a movement in the yaw direction could cause the flow angularity in pitch to change drastically, indicating that the probe was no longer directly above the vortex center where the pitch angle was nearly zero. Because of

the importance of knowing the relative position of the vortex center and probe in order to reduce the pressure data into velocity profiles and accurately find the core radius, it was decided not to move the probe in yaw or pitch while traversing the vortex. Thus the disturbance of the vortex was minimized.

Vortex probe interaction was studied at some length during the preliminary investigations. Observations of probe-vortex interaction made using tuft grids and probes indicated that the probe used did not alter the vortex significantly as long as the probe was parallel to the vortex core. A study of probe yaw and pitch effects on the vortex indicated vortex movement of up to 10% of the core radius at large pitch and yaw angle combinations. Simple potential theory gives a repulsive force between the vortex and probe in the outer vortex of  $F = -[\rho \Gamma^2 a^2 / 2\pi r(r^2 - a^2)]$ . However, it was found that if the probe is not rotated in the area of the core the interaction can be minimized and produces negligible effects in the calculation of the final experimental results.

Static pressure measurement presented a similar problem in that measurements had to be made with the probe aligned with the local flow direction. Therefore the static probe was much smaller in projected side area than the yawhead probe and it was assumed that the disturbance of the vortex due to the static probe moving in yaw was negligible. It was found possible to make the static pressure measurements using the static probe only in the case of mass injection due to the low flow angles and gradients involved in the mass injection case. For the normal trailing vortex it was found that the static probe could not be aligned in the flow with adequate confidence and centerline total head minus freestream static measurements could not be adequately duplicated at the same positions. Thus, Winternitz<sup>10</sup> method for determining static pressure from the yawhead probe was used. This method involves some additional probe calibration. Use of Winternitz method showed consistent results with the pressure predicted from inviscid considerations and high repeatability, and the results from this method in the area of the centerline were used to key the inviscid theory for static pressure distribution. Tests were conducted at 10, 15, 20, 25, and 30 chordlengths downstream of the wing at dynamic pressures of 1 and 2 in. of water. Effects of mass injection were investigated at 10, 20, and 30 chordlengths downstream. For the purpose of simplifying data reduction, it was assumed that the vortex path was parallel to the freestream path. This is consistent with earlier work<sup>11</sup> showing that after a distance of a few chordlengths downstream of the wing the vortex travels parallel to the freestream. This study does not make any conclusions as to the path of the vortex due to the effects of the tunnel walls, however in the analysis of flow properties at particular stations it is assumed that the wall has no effect. This seems justified since the vortex core is at least 24 core diameters from the nearest wall. Any pressure gradient in the freestream direction would have an effect on the vortex but the Virginia Tech Six-Foot Tunnel has a negligible pressure gradient throughout the entire test section. In addition, the flow at the extreme test section front was found to be uniform, and wind tunnel corrections on the wing properties were found to be negligible.

Initial experimental results which had been obtained assuming a constant static pressure distribution, showed very high circumferential velocities. Examination of the radial momentum equation shows that if  $V_\theta$  is large, then  $\partial P / \partial r$  cannot be negligible. Because the yawhead probe was calibrated in a uniform stream for  $\Delta P / Q$  indicated, it was difficult to decide what the proper indicated dynamic pressure for initial data reduction should be. Preliminary work indicated that there was a slight velocity excess in the core and thus it was assumed that the dynamic pres-

sure to use initially was that of the freestream. Using this dynamic pressure the initial flow angularities were calculated. Using these angularities the static pressure probe traverse was made. Then using the correct static pressure distribution, the final dynamic pressure and flow angularities could be calculated. This was possible because inspection of the static probe calibration shows negligible error for misalignment angles less than  $4^\circ$ , and none of the corrected angles were more than  $3^\circ$  different than the initial angle.

From Bernoulli's incompressible equation

$$P_o = 1/2\rho V^2 + P_{st} \quad (1)$$

the total velocity  $V$ , can be calculated from

$$V = (\{2[(P_o - P_{st\infty}) - (P_{st} - P_{st\infty})]\}/\rho)^{1/2} \quad (2)$$

where  $(P_{st} - P_{st\infty})$  could be obtained directly from the yawhead probe by the method of Winternitz.<sup>9,10</sup> Thus with the flow angularity known from probe calibration, and the velocity from Eq. (2), cylindrical component velocities  $V_\theta$ ,  $V_r$  and  $V_z$  were obtained using the center of the vortex as the origin, and the fact that the traverses were made on a vertical line through the origin.

With  $V_\theta$  known, the circulation  $\Gamma$ , can be calculated from  $\Gamma = 2\pi V_\theta r$ , where  $r$  is the distance from the vortex center defined as the location of  $V_\theta = 0$ .

From the experimental work it is seen that the vortex does exhibit a solid body rotation, and a simple expression for the variation of static pressure can be given by using the Rankine vortex model along with the experimental value of the core radius  $A_c$  which seems to be independent of the method of data reduction, and the experimental static pressure at the centerline. The resulting pressure distribution is

$$(P_\infty - P) = \rho\Gamma^2/8\pi^2 r^2 \text{ for } r > A_c \quad (3)$$

and

$$(P_\infty - P) = (\rho\Gamma^2/4\pi^2 A_c^2)(1 - r^2/2A_c^2) \text{ for } r \leq A_c \quad (4)$$

These relations can then be used to find detail pressure distributions, and for comparison with the experimental methods.

#### Theoretical Considerations and Investigation

An inviscid vortex model used by Betz<sup>9</sup> to describe the outer vortex for an elliptic wing has been generalized to include arbitrary wings and certain aspects of the viscous theories need to be discussed for comparison with experimental results. The essence of Betz's work is that the moment of inertia of the flat vorticity sheet immediately behind the wing about its center of gravity is identical to the moment of inertia of a circular vortex about its center after the sheet is fully rolled-up. For this calculation lifting line theory is assumed adequate and the various wings may be represented by different functions  $\Gamma(y)$ , where standard finite wing theory is used so that

$$\Gamma(y) = 4sV \sum_{n=1}^{\infty} A_n \sin n\theta$$

represents the true circulation with  $\theta = \cos^{-1}y/s$ . The  $A_n$  are calculated by use of the monoplane equation in the present work. Note that the immediate downstream vorticity sheet strength is given by  $\gamma(y)$ , and it is related to  $\Gamma$  by  $\gamma(y) = -[d\Gamma(y)/dy]$ . The c.g. of the undeveloped sheet is

$$\bar{y}_1 = \int_{y_1}^s y \left( \frac{-d\Gamma(y)}{dy} \right) dy / \int_{y_1}^s \frac{-d\Gamma}{dy} dy$$

which can be given in terms of the standard wing variable

as

$$\bar{y}_1 = \frac{s}{\Gamma(y_1)} \int_0^{\theta_1} \cos\theta \frac{d\Gamma}{d\theta} d\theta$$

Similarly the moment of inertia about  $y = 0$  can be given by

$$J_o(y_1) = s^2 \int_0^{\theta_1} \cos^2\theta \frac{d\Gamma}{d\theta} d\theta$$

which is related to the moment of inertia about the c.g. by

$$J_y = J_{oy_1} - \Gamma_y \bar{y}_1^2 \quad (5)$$

Instead of immediately assuming a value of  $\Gamma$  as did Betz, the analysis can remain general and, if the argument of Betz is repeated in this manner, a more general relationship showing the effect of various wings can be found. At some point  $r_1$  the circulation will be the same as at a point on the wing,  $\Gamma_{r1} = \Gamma_{y1}$ , but the relation between  $y_1$  and  $r_1$  is not yet known. This is found by use of the moment of inertia restriction,  $J_{r1} = J_{y1}$ .

Permitting  $r$  to increase by  $dr$ , then  $y$  decreases by  $dy$  and  $\theta$  increases by  $d\theta$  under these premises. The result is an increase in circulation of

$$(\partial\Gamma_r/\partial r)dr = (\partial\Gamma_y/\partial\theta)d\theta$$

and in inertia moment of

$$(\partial\Gamma_r/\partial r)r^2 dr = (\partial J_y/\partial\theta)d\theta$$

where  $\partial J_y/\partial\theta$  is known from Eq. (5). Finally, combining the above relations,

$$r^2 = \frac{\partial J_y/\partial\theta}{\partial\Gamma_y/\partial\theta} \quad (6)$$

and the relation between  $r$  and  $y$  is now known. These results have been used for calculations using various wing planforms, and the results are given in the next section.

The detailed computational aspects of the above analysis have been given in Ref. 12. An example, showing the effect of the generalized analysis is given in Fig. 4.

Rinehart<sup>13</sup> has shown the effect of mass injection on the circumferential velocity distribution using the axial velocity profiles from the theory of Batchelor.<sup>14</sup> As will be seen, his results are in qualitative agreement with experiment.

Finally, McCormick<sup>15</sup> has given an empirical prediction of the circumferential velocity distributions based on flight test data which can be compared to the wind-tunnel data in order to assess the possibility of using the wind tunnel to simulate full-scale conditions. This result is based on a logarithmic distribution of circulation in the area of the core radius. It is interesting to note that for rectangular wings the inviscid theory discussed above also predicts a very nearly linear distribution of circulation clouding the implications of this logarithmic calculation distribution.

#### Results and Discussion

Typical results of the theoretical investigation for several types of wings are shown in Figs. 5 and 6. The conclu-

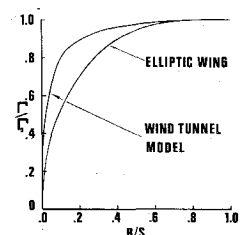


Fig. 4 Generalized solution.

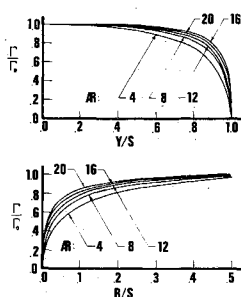


Fig. 5 Circulation distribution for various aspect ratios.

sion to be drawn is that the vortex will become more intense as the circulation is concentrated on the outer portion of the wing. This provides theoretical verification of several experimental observations. Garodz<sup>16</sup> has concluded that the vortex is much less intense when originated by a wing configuration in which flaps are deflected. Smith<sup>17</sup> has also shown that the vortex is much less intense if a porous wing tip is used. It is certain that in such cases the circulation is concentrated near the wing root. Therefore it appears that any configuration that generates the major portion of the lift near the wing root will minimize the trailing vortex disturbance.

For the wind-tunnel case the agreement between experiment and theory is shown in Fig. 7. These results can also be compared to the experimental work of Grow<sup>18</sup> who concluded that the core size seemed to remain independent of aspect ratio and become larger as the taper ratio increased, while the maximum tangential velocity increases with both aspect ratio and taper. This is entirely consistent with the theoretical results of Figs. 5 and 6, which show increases in the predicted inviscid circulation in the area of the vortex center. This comparison with experimental results also seems to warrant the general conclusion that even though the inviscid theory does not predict a maximum tangential velocity, it does seem to imply that for a fixed root circulation  $\Gamma_0$ , maximum tangential velocity will become larger as the major portion of the vorticity is shed near the wing tip. Finally, it seems that Garodz's observation that some smaller aircraft (e.g., DC-9) with very "clean" wing configurations produce very intense vortices, is also compatible with the theoretical predictions.

Experimental results can now be analyzed. It should be noted that although runs were made for the modified wing with no blowing at each station, the differences between these results and the results of runs with the clean wing at the same station were considerably smaller than the expected experimental error. The results of principal interest are the tangential and axial velocities and the static pressure and circulation distributions. The radial velocity is a second order term and is more subject to experimental error since, if the traverse is not made perfectly, the radial velocity will contain contributions from the other velocity components which will be of the same order as the radial velocity. Therefore, the radial velocity has been tabulated along with a complete data in Ref. 11, but is not presented here.

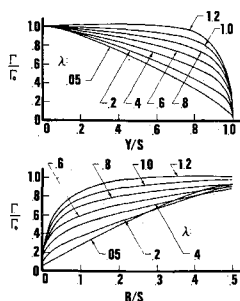


Fig. 6 Circulation distribution for various taper ratios.

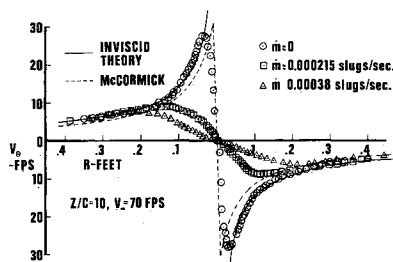


Fig. 7 Tangential velocity profiles  $Z/C = 10$ ,  $V = 70$  fps.

The tangential velocity profiles are plotted for each case in the conventional manner. Each figure contains the inviscid prediction based on the present theory, and an empirical prediction proposed by McCormick.<sup>15</sup>

Examination of vortex tangential velocity profiles (Figs. 7-12) shows good agreement with the inviscid theory and adequate correlation with the flight test derived empirical equation. It is seen that as the vortex moves downstream there is very little decay.

Note that as the vortex moves downstream the outer portion of the vortex "widens." This must be the initial effect of viscous decay.

The effect of mass injection for two downstream stations at  $V = 70$  fps is shown in Figs. 7 and 8. Examination of these figures show the drastic effect of mass injection on the tangential velocity. It is important to notice that the profiles converge to the zero mass injection case for the outer portion of the vortex, showing that the total amount of circulation in the vortex has not been changed but that the vorticity has been distributed over a larger area. The trend of larger core radius and low tangential velocities seems to be continuing as the vortex moves downstream. Figure 13 shows the effect of mass injection on the characteristic core parameters  $V_{\theta \max}$  and  $A_c$  at  $z/c = 30$ . This result is in agreement with the work of Rinehart,<sup>13</sup> who predicted these effects from analytical considerations. Poppleton<sup>19</sup> observed less effect of mass injection, but with a more intense vortex generated by a split wing.

It appears that the effect of mass injection is primarily that of introducing large amounts of turbulence into the core area during formation of the vortex, resulting in large eddies that help diffuse the vorticity. If this is the case it is then possible that any method which would cause large amounts of turbulence to be generated in the area of the wing tip would have an equivalent effect.

Examination of the axial velocities,  $V_z$  (Figs. 14 and 15) shows that for the  $V = 70$  fps case even with no mass injection there is no large excess or deficit, and it is difficult to detect a trend. In the  $V = 100$  fps case the results indicate an overshoot in velocity of almost 10% near the location of maximum tangential velocity. This is in contrast to the previously assumed behavior (Refs. 2 and 3). In the mass injection case (Fig. 14) the effect of the jet is not as pronounced as might be expected. Indeed in the full injection case at far downstream stations the axial velocity on the axis is less than in the moderate blowing case. The chief effect of full mass injection is to "fill out"

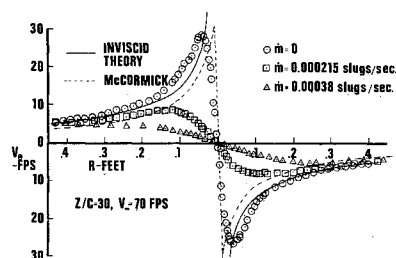
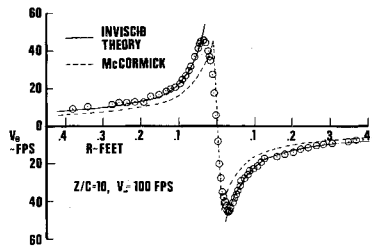


Fig. 8 Tangential velocity profiles  $Z/C = 30$ ,  $V = 70$  fps.

Fig. 9 Tangential velocity profiles  $Z/C = 10$ ,  $V = 100$  fps.



the velocity profile. It is possible to understand this phenomenon by noting the coupling effect with which the tangential velocity governs the pressure distribution in the vortex, which in turn governs the axial velocity distributions. Thus, as the increase in injection decreases the maximum tangential velocity, the static pressure deficit in the vortex is reduced and the axial velocity appears to lose the large velocity excess that would appear if there were no swirl.

The static pressure distributions obtained is shown in Figs. 16 and 17. It should be recalled that the theoretical curve [Eq. (3) and (4)] was used to reduce the data in the case of zero mass injection. It can readily be seen that the use of the theory is justified by the excellent correlation of the data, where the theory has been keyed to the experimental data at the centerline.

Figures 18 and 19 are typical circulation distributions. It is easily seen that in general the data follows the theoretical prediction. Exceptions are the core region circulation deficiency, the circulation "overshoot" immediately outside the core, and the region far from the core which shows a large degree of data scatter. It is also observed that even at distances of 10 core radii the circulation is still far from the value at the wing root. In the light of the present theory this is to be expected. Previous investigators have obtained similar results, but were unable to explain the results. For the present work at  $V = 70$  fps,  $\Gamma_{AC}/\Gamma_o = 0.46$  and for  $V = 100$  fps,  $\Gamma_{AC}/\Gamma_o = 0.40$ . This is much lower than the predicted value of 0.72 for laminar viscous theory.

The circulation near the center of the vortex is that expected for a solid body type rotation. At distances of  $A_c$  and slightly greater from the core the circulation overshoots the predicted inviscid circulation values. This would be expected from examination of the tangential velocity profiles. Donaldson<sup>20</sup> has noted this behavior previously in a more restrictive class of theoretical examinations which did not account for the inviscid circulation given by the method of Betz. His results showed that this only occurred in turbulent flows. This would seem to indicate that the primary turbulence effect is to "pull" more at the fluid along with the core than would be expected. Indeed, this leads to the image of a circular cylinder placed in an external circulation field and suddenly set in rotation (Rayleigh problem). The result would be an increase of tangential velocity which would be added to the inviscid external tangential velocity. This would cause the circulation to overshoot the value in the area of the core. In the region far from the core there is a large degree of data scatter. This would be a result of magnification of

Fig. 10 Tangential velocity profiles  $A/C = 30$ ,  $V = 100$  fps.

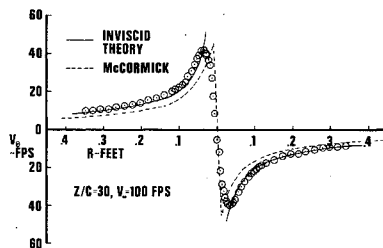


Fig. 11 Decay of  $V_{\theta_{max}}$ .

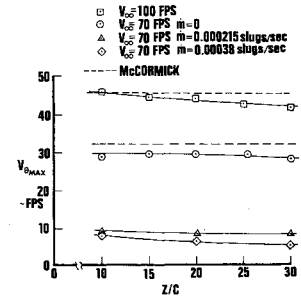


Fig. 12 Change of core radius with  $Z/C$ .

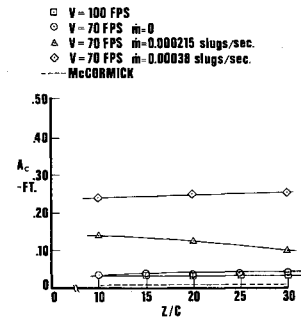


Fig. 13 Core parameter change with mass injection  $V = 70$  fps,  $Z/C = 30$ .

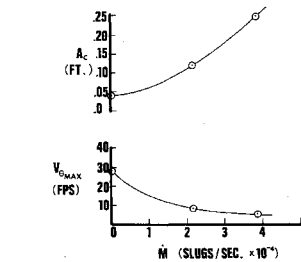


Fig. 14 Axial velocity profiles,  $V = 70$  fps.

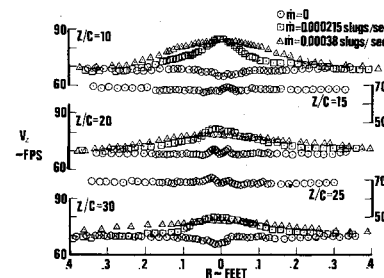


Fig. 15 Axial velocity profiles,  $V = 100$  fps.

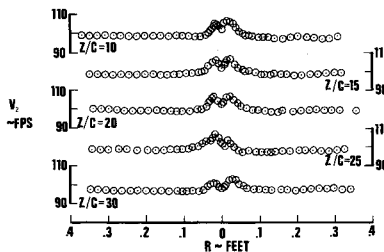
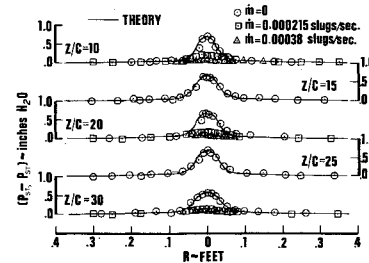


Fig. 16 Static pressure profiles  $V = 70$  fps.



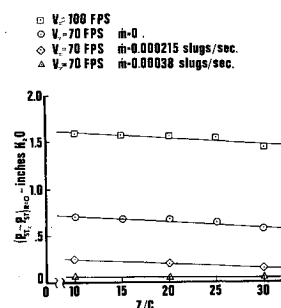


Fig. 17 Decay of centerline static pressure deficit.

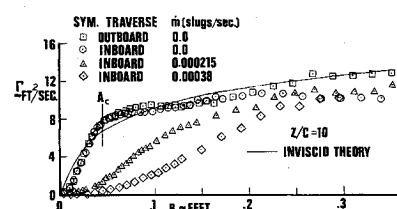


Fig. 18 Typical circulation distribution,  $V = 70$  fps.

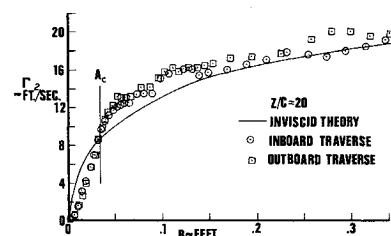


Fig. 19 Typical circulation distribution,  $V = 100$  fps.

experimental error in the farfield. It seems that the error inherent in the long times for settled values and the small changes in reading for each point far from the core could easily result in the high amount of data scatter. Note that good symmetry is shown in the area of the core. The effects of mass injection are clear in Fig. 20. It is seen that the value of the circulation is approaching the expected inviscid prediction and that the circulation is not destroyed by the mass injection.

### Conclusions

A vortex was generated in the Virginia Tech Six-Foot Subsonic Wind Tunnel and it has been found possible to use a probe to investigate the detailed structure of the mean flowfield of the vortex over the entire test section length. Summarizing the detailed findings: it is concluded that the axial velocity does not show the large deficits (50%) reported previously, tangential velocities were found to be higher than the near wing velocities found by Chigier and to show a much smaller rate of decay than the value predicted by standard viscous theory. This supports the present prediction method since Chigier used a low aspect ratio wing. Also, the core diameter has been found to be approximately 12% of the wing chord and essentially constant as the vortex travels downstream, in agreement with the near wing work of Gasperek and Chi-

gier. Mass injection at the wing tip has been shown to be an effective means of destroying the high peak tangential velocities in the vortex through the introduction of large scale turbulence into the core area.

It has been concluded that the generalization of the method of Betz has been shown to fit the outer portion of the experimental vortex excellently, and that the vortex becomes more intense as the majority of vorticity is shed near the wing tip, simulating a single line vortex.

### References

- 1 Fage, A. and Simmons, L. F. G., "An Investigation of the Air-Flow Patterns in the Wake of an Aerofoil of Finite Span," *Philosophical Transactions of the Royal Society*, Vol. A225, 1925, p. 303.
- 2 Mowforth, E., "Details of Measurements in a Turbulent Trailing Vortex," *Aeronautical Quarterly*, May 1959, p. 161.
- 3 Gasperek, E., "Viscous Decay of a Vortex," Master's thesis, 1960, Mechanical Engineering Dept., Syracuse Univ., N. Y.
- 4 Chigier, N. A. and Corsiglia, V. R., "Tip Vortices-Velocity Distributions," Preprint 522, presented at the 27th Annual National V/STOL Forum of the American Helicopter Society, Washington, D. C., May 1971.
- 5 Squire, H. B., "The Growth of a Vortex in Turbulent Flow," ARC 16,666, 1954, Aeronautical Research Council, England; also *Aeronautical Quarterly*, Aug. 1965, p. 302.
- 6 Fernandez, F. L. and Lubard, S. C., "Turbulent Vortex Wakes and Jets," AIAA Paper 71-615, Palo Alto, Calif., 1971.
- 7 Hoffman, E. R. and Joubert, P. N., "Turbulent Line Vortices," *Journal of Fluid Mechanics*, Vol. 16, Pt. 3, July 1963, p. 395.
- 8 Donaldson, C. duP., "A Brief Review of the Aircraft Trailing Vortex Problem," A.R.A.P. Rep. 155, May 1971, Aeronautical Research Associates of Princeton, Princeton, N. J.
- 9 Betz, D., "Behavior of Vortex Systems," T.M. 713, June 1933, NACA.
- 10 Winternitz, F. A. L., "Probe Measurements in Three-Dimensional Flow," *Aircraft Engineering*, Vol. 28, No. 330, Aug. 1956, p. 273.
- 11 Mason, W. H. and Marchman, J. F., "Investigation of an Aircraft Trailing Vortex Using a Tuft Grid," College of Engineering, VPI-E-71-17, Aug. 1971, Virginia Polytechnic Inst. and State Univ. Blacksburg, Va.
- 12 Mason, W. H., "Farfield Structure of an Aircraft Trailing Vortex, Including Effects of Mass Injection," Masters thesis, Nov. 1971, Aerospace Engineering Dept., Virginia Polytechnic Inst. and State Univ., Blacksburg, Va.
- 13 Rinehart, S. A., "Effects of Modifying a Rotor Tip Vortex by Injection on Downwash Velocities, Noise and Airloads," presented at Joint Symposium on Environmental Effects on VTOL Designs, Arlington, Texas, Nov. 1970.
- 14 Batchelor, G. K., "Axial Flow in Trailing Line Vortices," *Journal of Fluid Mechanics*, Vol. 16, Pt. 3, Dec. 1964, p. 645.
- 15 McCormick, B. W., "Aircraft Wakes: A Survey of the Problem," presented at the FAA Symposium on Turbulence, Washington, D. C., March 22-24, 1971.
- 16 Garodz, L. J., "Federal Aviation Administration Full-Scale Aircraft Vortex Wake Turbulence Flight Test Investigations: Past, Present, Future," AIAA Paper 71-97, New York, 1971.
- 17 Smith, H. C., "Effects of a Porous Wingtip on an Aircraft Trailing Vortex," M. S. thesis, Dec. 1967, Dept. of Aerospace Engineering, The Pennsylvania State Univ., University Park, Pa.
- 18 Grow, T. L., "The Effect of a Wing on a Tip Vortex," *Journal of Aircraft*, Vol. 6, No. 1, Jan.-Feb. 1969, p. 37.
- 19 Popleton, E. D., "Effect of Air Injection into the Core of a Trailing Vortex," *Journal of Aircraft*, Vol. 8, No. 8, Aug. 1971, p. 672.
- 20 Donaldson, C. duP., "Calculation of Turbulent Shear Flows for Atmospheric and Vortex Motions," AIAA Paper 71-217, New York, 1971.